An Internal Model Approach to Robust Current Control of IPMSM Drives with Respect to Unknown and Varying Inductances

René Metzkow [*] **Juan G. Rueda-Escobedo** [*] **Daniela Döring** [**] **Johannes Schiffer** [*]

[*] *Fachgebiet Regelungssysteme und Netzleitechnik, Brandenburgische Technische Universität Cottbus - Senftenberg (e-mail: {metzkren,ruedaesc,schiffer}@b-tu.de)*
[**] *Fachgebiet Systemtechnik, Brandenburgische Technische Universität Cottbus - Senftenberg (e-mail: daniela.doering@b-tu.de)*

Abstract: Interior permanent magnet synchronous machines (IPMSMs) are well-suited for high-performance applications, such as traction drives in hybrid and electric vehicles. Yet a major challenge to fully exploit their potential is the fact that their self and cross-coupling inductances vary significantly across the operation range. In addition, this variation is difficult to characterize and complicates the design of provably stabilizing and robust controls. Motivated by this, by using an IPMSM model with current dependant inductances together with the internal model principle, a nonlinear current control scheme is derived that renders the equilibrium point of the closed-loop system exponentially stable. Both the control and the stability result only require the knowledge of an upper bound of the gradient of the inductances as well as lower and upper bounds on the inductance values themselves, while their actual evolution can be completely unknown. This is a major advantage compared to existing (PI-based) current control approaches, as it makes costly practices to determine the inductance variations unnecessary. The efficacy of the proposed control scheme is demonstrated in a simulation example.

Keywords: Permanent magnet motors, Two-axis machine model, Electric machines, Internal model principle, Robustness

1. INTRODUCTION

Hybrid electric vehicles as well as electric vehicles represent a highly promising alternative to conventional automobiles on the path to a carbon-free society (Mou et al., 2019). Hence, electric machines tend to replace traditional internal combustion engines in the near future. In these emerging applications, an efficient and compact electric machine is needed in order to increase the autonomy of the vehicles. A machine type which is of particular interest in this setting is the interior permanent magnet synchronous machine (IPMSM) (Sulaiman et al., 2011). Compared to conventional induction and switched-reluctance machines, IPMSMs offer a series of advantageous characteristics, such as high efficiency, high-torque/power density, high torque-to-inertia ratio and absence of rotor losses (Zhu and Howe, 2007; Zaky, 2011; Chan and Chau, 2001; Momoh and Omoigui, 2009). These properties paired with the urgent need to decarbonize the transportation sector have led to great interest in the improvement of the IPMSM operation and control (Carpiuc et al., 2011; Zaky, 2011; Liu et al., 2018).

An inherent property of the IPMSM is its significant degree of saliency compared to the surface mounted permanent magnet synchronous machine (SPMSM). This saliency allows to use the reluctance torque (Blaschke, 1972), which is not possible in the SPMSM, and enables the possibility of operating the machine at higher speeds by using the field weakening method (Blaschke, 1972).

However, a major difficulty in the control of the IPMSM is the significant variation of the machine inductances over different operation regions. For instance, it has been reported in (Stumberger et al., 2003) that the cross-coupling inductances can reach up to 40% of the nominal value of the self-inductance in both axes, making these variations nonnegligible. An additional challenge is that the variation of the inductances is very difficult to characterize (Liang et al., 2016). These facts complicate the full exploitation of the machine's capabilities (Liang et al., 2016).

A common way to approach this issue is by performing extensive tests on the machines, in order to build look-up-tables (LUTs) that are then used for the control implementation (Wallscheid et al., 2012; Yu et al., 2017). A different approach is to obtain the machine parameters via numerical simulations based on the finite element method (FEM) (Meessen et al., 2008; Gyu-Hong Kang et al., 2000). Yet, both approaches have severe drawbacks in common: The characterization has to be done machine-wise, which

is time consuming and expensive in the case of the experiments. In addition, the parameters may change during the machine's lifetime.

These parameter variations are of particular relevance in the standard dq-based current control scheme, which uses an inductance-dependant feed-forward term to eliminate the cross-couplings between the machine axes (Du and Yu, 2007; Liu et al., 2018). Clearly, this feed-forward decoupling is very sensitive to inductance variations. As a consequence, it is highly desirable to develop a control law that requires minimal information on the machine parameters. This problem is tackled in the present paper.

At the core of the proposed approach is the observation that - while the standard model of the IPMSM relates the cross-coupling terms in the machine dynamics directly to the machine inductances - any model derived from first-principles, see e.g. (Stumberger et al., 2003), shows that this term in fact depends on the flux-linkage. By recognizing and using this relation, the present paper contains the following three contributions:

(1) Based on the internal model principle (Francis and Wonham, 1976; Jie Huang and Ching-Fang Lin, 1993), a nonlinear current control is proposed, which includes a dynamical compensator for the flux-linkage dependant cross-coupling term. As a consequence its implementation does not require any knowledge on the inductances nor their variations during the operation.

(2) Local exponential stability of the resulting closed-loop equilibrium as well as robustness with respect to unknown and varying inductances is established. The latter is a direct consequence of using the internal model principle in the control design. In addition, it is shown that the region for which the convergence of the error is ensured, can be estimated by a ball, whose radius increases inversely proportional to the rate of change of the machine inductances. Hence, for the nominal scenario with constant machine inductances even global stability is guaranteed. To establish these results, the inductance matrix merely has to satisfy some qualitative properties, i.e., it has to be symmetric, positive definite and uniformly bounded. All these properties are fulfilled in any practical scenario.

(3) A comparison between the tracking performance of the proposed control and the conventional PI-control is provided via numerical simulation.

In summary, under the abovementioned mild conditions and unlike previous approaches in the literature (Carpiuc et al., 2011; Lemmens et al., 2015), the proposed controller ensures exponential tracking of constant current references without having any precise knowledge of the machine inductances.

The structure of the paper is as follows. In Section 2, the model of the IPMSM is introduced together with the control design based on the internal model principle. The main properties of the proposed control are established in Section 3. In Section 4, a simulation example is provided to illustrate the properties of the proposed control and its performance is compared with that of the standard PI approach (Du and Yu, 2007; Liu et al., 2018). Finally,

the proofs of the claims made in Section 3 are given in Appendix A.

Notation: Along the note, $\mathbb{R}$ denotes the set of real numbers, $\mathbb{R}^n$ the real n-dimensional Euclidean space and $\mathbb{R}^{n \times m}$ the set of real matrices. $\mathbf{I}_n \in \mathbb{R}^{n \times n}$ denotes the identity matrix. Also, $\mathbf{J} \in \mathbb{R}^2$ denotes the matrix imaginary unit $\begin{bmatrix} 0 & 1 \\ -1 & 0 \end{bmatrix}$. For symmetric matrices $A \in \mathbb{R}^{n \times n}$ and $B \in \mathbb{R}^{n \times n}$, $A > B$ ($A \geq B$) means that $A - B$ is positive (semi)definite. For $v \in \mathbb{R}^n$, $\|v\| = (v^\top v)^{1/2}$ denotes the Euclidean norm and for $B \in \mathbb{R}^{m \times n}$, $\|B\|$ denotes the induced Euclidean norm of B, defined as $\sup_{\|x\|=1} \|B\,x\|$.

2. IPMSM MODEL AND CONTROL DESIGN

2.1 IPMSM Model

The dynamical model of the electrical part of the IPMSM in dq-coordinates is given in terms of the flux linkage $\lambda_{dq}(t) \in \mathbb{R}^2$ by (Pillay and Krishnan, 1988; Schröder, 2015)

$$\dot{\lambda}_{dq}(t) = u_{dq}(t) - r_s i_{dq}(t) + \omega_{\text{el}}(t)\mathbf{J}\lambda_{dq}(t), \qquad (1)$$

where $r_s > 0$ represents the stator resistance, $u_{dq}(t) \in \mathbb{R}^2$ represents the motor voltage, i.e., the control signal, and $i_{dq}(t) \in \mathbb{R}^2$ represents the motor current, whereas $\omega_{\text{el}}(t) \in \mathbb{R}$ represents the electrical angular velocity. Since almost any machine is fitted with a proper cooling system, assuming the resistance r_s to be constant is reasonable (Gai et al., 2018).

The dynamics of the IPMSM's mechanical part is given by

$$J \frac{\mathrm{d}}{\mathrm{d}t} \omega_{\text{mech}}(t) = T_E(t) - T_L(t) - \beta \omega_{\text{mech}}(t). \qquad (2)$$

Here, $T_E(t) \in \mathbb{R}$ denotes the electrical torque defined as

$$T_E(t) = \frac{3p}{2}\Big(\lambda_{dq}(t) \times i_{dq}(t)\Big), \qquad (3)$$

where $\times$ denotes the vector cross product and $p > 1$ represents the number of poles. Furthermore, $T_L(t) \in \mathbb{R}$ is the load torque, $J > 0$ is the rotor moment of inertia, $\beta > 0$ is the viscous friction coefficient and $\omega_{\text{mech}}(t) \in \mathbb{R}$ corresponds to the mechanical angular velocity, which is related to the electrical angular velocity by $p\,\omega_{\text{mech}}(t) = \omega_{\text{el}}(t)$.

The model (1) contains two variables, namely $\lambda_{dq}(t)$ and $i_{dq}(t)$. However, it is common practice to have a model just in terms of the current (Schröder, 2015). Obtaining such model is possible since there is an algebraic relation that links $\lambda_{dq}(t)$ to $i_{dq}(t)$ (Pillay and Krishnan, 1988; Schröder, 2015). The usual way of establishing the latter is by assuming a linear relation between the variables plus a bias term, which represents the flux linkage established by the permanent magnets (Carpiuc et al., 2011; Ortega et al., 2018):

$$\lambda_{dq}(t) = L_{dq}i_{dq}(t) + \lambda. \qquad (4)$$

It is important to stress that the inductance matrix $L_{dq} \in \mathbb{R}^{2 \times 2}$ and the bias term $\lambda \in \mathbb{R}^2$ are assumed to be constant. Furthermore, the inductance matrix is usually assumed to be symmetric and positive definite, i.e., $L_{dq} = L_{dq}^\top > 0$, with

$$L_{dq} = \begin{bmatrix} \ell_{dd} & \ell_{dq} \\ \ell_{qd} & \ell_{qq} \end{bmatrix},$$

where $\ell_{dd} > 0$ and $\ell_{qq} > 0$ denote the self inductances and $\ell_{dq} \geq 0$ and $\ell_{qd} \geq 0$ denote the cross-coupling inductances.

By combining (1) and (4) one obtains the electrical IPMSM dynamics purely in terms of the current, i.e.,

$$L_{dq}\frac{\mathrm{d}}{\mathrm{d}t}i_{dq}(t) = u_{dq}(t) - r_s i_{dq}(t) \\ + \omega_{\mathrm{el}}(t)\mathbf{J}\left(L_{dq}i_{dq}(t) + \lambda\right). \tag{5}$$

The model (5) is accurate enough, when the IPMSM works locally around a specific operation point. However, phenomena like anisotropy and saturation require to use different values of L_{dq} for different operation points. This problematic has been widely recognized for the IPMSM (Li et al., 2017; Kim et al., 2018; Sun et al., 2018).

Experimentally it has been shown that the flux linkage can be represented as a smooth function of the machine currents (Stumberger et al., 2003). Let $\phi : \mathbb{R}^2 \to \mathbb{R}^2$ denote this function, then

$$\lambda_{dq} = \phi(i_{dq}), \qquad \phi^\top(i_{dq}) = \left[\phi_1(i_{dq})\ \phi_2(i_{dq})\right]. \tag{6}$$

By using this function, the inductances of the machine can be defined on the basis of the work in (Stumberger et al., 2003; Li et al., 2017) as follows:

$$\ell_{dd}(i_{dq}) = \frac{\partial \phi_1}{\partial i_d}(i_{dq}), \qquad \ell_{dq}(i_{dq}) = \frac{\partial \phi_1}{\partial i_q}(i_{dq}),$$

$$\ell_{qd}(i_{dq}) = \frac{\partial \phi_2}{\partial i_d}(i_{dq}), \qquad \ell_{qq}(i_{dq}) = \frac{\partial \phi_2}{\partial i_q}(i_{dq}).$$

Clearly the Jacobian matrix of ϕ plays the role of the inductance matrix, i.e.,

$$L_{dq}(i_{dq}) = \frac{\partial \phi}{\partial i_{dq}}(i_{dq}). \tag{7}$$

Common assumptions on $L_{dq}(i_{dq})$ are that it is symmetric, positive definite and bounded for all $i_{dq}(t)$ (Gyu-Hong Kang et al., 2000; Lee et al., 2019), as stated in the assumption below.

Assumption 1. The inductance matrix $L_{dq}(i_{dq})$ given in (7) satisfies $L_{dq}(i_{dq}) = L_{dq}^\top(i_{dq})$ and $\alpha_1 \mathbf{I}_2 \geq L_{dq}(i_{dq}) \geq \alpha_2 \mathbf{I}_2 > 0$, for some positive constants $\alpha_1 \geq \alpha_2 > 0$ and for all $i_{dq} \in \mathbb{R}^2$.

By replacing λ_{dq} with $\phi(i_{dq})$ in (1), one obtains the model

$$L_{dq}(i_{dq}(t))\frac{\mathrm{d}}{\mathrm{d}t}i_{dq}(t) = u_{dq}(t) - r_s i_{dq}(t) \\ + \omega_{\mathrm{el}}(t)\mathbf{J}\,\phi(i_{dq}(t)), \tag{8}$$

which forms the basis for the control design in the present paper and compared to (5) takes the variation of the inductances explicitly into account.

2.2 An Internal Model Approach to Robust Current Control Design for the IPMSM

For speed regulation in synchronous motors, it is common practice to have a cascade control (Choi et al., 2019; Hosseini and Tabatabaei, 2017), where the outer-loop regulates the machine speed and generates references for the currents, which have to be tracked by the controller in the inner-loop. By following this standard paradigm, in the present paper paper the focus is on the design of a robust inner-loop current control for the IPMSM in the presence of varying and unknown inductances. This objective is formalized below.

Problem 2. Consider the system (8) with Assumption 1. Assume that the electrical angular frequency $\omega_{\mathrm{el}}(t)$ is measured. Let $i_{dq}^{\mathrm{ref}} \in \mathbb{R}^2$ be a constant vector. Design a control law for the input $u_{dq}(t)$ that guarantees

$$\lim_{t\to\infty} \|i_{dq}^{\mathrm{ref}} - i_{dq}(t)\| = 0.$$

For a constant inductance matrix, a PI-control can be used as current controller (Du and Yu, 2007; Liu et al., 2018). This typically involves a feed-forward term to cancel the influence of the cross-coupling term $\omega_{\mathrm{el}}(t)\mathbf{J}(L_{dq}i_{dq}(t) + \lambda)$ in (5). However, the implementation of this term requires precise knowledge of L_{dq} and λ. Furthermore, as illustrated via simulation in Section 4, in the presence of a varying inductance matrix this type of PI-based-control will exhibit a steady-state error when trying to solve Problem 2 as soon as the inductance matrix deviates from its nominal value. A similar feed-forward approach could be used, if an accurate characterization of $\phi(i_{dq})$ was available. However, obtaining such characterization involves intensive testing on the machine, and even after this, there is no guarantee that ϕ will not change during the operation of the machine.

Therefore, instead of further characterizing ϕ, we propose to understand it as a disturbance, for which a dynamical model is available, i.e., (1). By recognizing this fact and by using the internal model principle, we propose a dynamic state feedback controller of the form

$$u_{dq}(t) = -k_1 e_1(t) + r_s i_{dq}^{\mathrm{ref}} - \omega_{\mathrm{el}}(t)\mathbf{J}z(t), \tag{9}$$

$$\dot{z}(t) = u_{dq}(t) - r_s i_{dq}(t) + \omega_{\mathrm{el}}(t)\mathbf{J}z(t) + \varphi(e_1(t)), \tag{10}$$

where $e_1(t)$ represents the reference tracking error, i.e.,

$$e_1(t) = i_{dq}(t) - i_{dq}^{\mathrm{ref}}.$$

The function φ in (10) is introduced to establish closed-loop stability and specified next. Furthermore, we define the dynamical compensation error as

$$e_2(t) = \phi(i_{dq}(t)) - z(t),$$

and the error vector as

$$e^\top(t) = [e_1^\top(t), e_2^\top(t)].$$

When (9) and (10) are used to control the system, they yield the error dynamics[1]

$$\dot{e}_1(t) = -L_{dq}^{-1}(t)\left((r_s + k_1)e_1(t) - \omega_{\mathrm{el}}(t)\mathbf{J}e_2(t)\right), \\ \dot{e}_2(t) = -\varphi(e_1(t)) + \omega_{\mathrm{el}}(t)\mathbf{J}e_2(t). \tag{11}$$

The error system (11) possesses an inherent skew-symmetric structure. In order to keep this structure, we propose to choose φ as a nonlinear feedback term of the form $\varphi(e_1(t)) = k_2\omega_{\mathrm{el}}(t)\mathbf{J}^\top e_1(t)$ with $k_2 > 0$. With this definition, the proposed controller (9) results in

$$u_{dq}(t) = -k_1 e_1(t) + r_s i_{dq}^{\mathrm{ref}} - \omega_{\mathrm{el}}(t)\mathbf{J}z(t), \\ \dot{z}(t) = u_{dq}(t) - r_s i_{dq}(t) + \omega_{\mathrm{el}}(t)\mathbf{J}z(t) \\ + k_2\omega_{\mathrm{el}}(t)\mathbf{J}^\top e_1(t). \tag{12}$$

Furthermore, with this choice of φ, the error dynamics can be written as

---

[1] To simplify the notation and whenever clear from the context, the explicit dependance of the inductance matrix L_{dq} on the motor currents i_{dq} is omitted in the sequel.

$$\dot{e}(t) = A(t)e(t),$$
$$A(t) = \begin{bmatrix} -L_{dq}^{-1}(t)(r_s + k_1) & \omega_{el}(t)L_{dq}^{-1}(t)\mathbf{J} \\ -k_2\omega_{el}(t)\mathbf{J}^\top & \omega_{el}(t)\mathbf{J} \end{bmatrix}. \qquad (13)$$

Clearly, $e(t) \equiv 0$ is an equilibrium point of the dynamics (13). Hence, it is shown in the next section that the proposed control (12) provides a solution to Problem 2 by establishing exponential stability of the origin of the error system (13).

3. STABILITY AND ROBUSTNESS PROPERTIES OF THE PROPOSED CONTROLLER

The controller proposed in (12) does not require explicit knowledge of the inductances. Instead of a precise characterization of the flux linkage in terms of the current, the controller in (12) uses a dynamic compensator to cancel the effect of the cross-coupling term $\omega_{el}(t)\mathbf{J}\phi(i_{dq}(t))$. This, in turn, grants the controller with robustness against variations in the inductances, a claim which is rigorously established in Theorem 6 below and also illustrated in Section 4 via simulation.

To prove this important property the inductances may not change arbitrarily fast. This requirement is reflected in Assumption 3, which implies that the inductances change smoothly with the current, something that can be expected in an IPMSM (Stumberger et al., 2003; Li et al., 2017).

Assumption 3. The gradient with respect to the current of the inductances $\ell_{ij}(i_{dq})$, with i, j denoting either d or q, is uniformly bounded by a constant, i.e.,
$$\left\| \frac{\partial \ell_{ij}}{\partial i_{dq}} \right\| \leq \bar{\ell}, \quad \bar{\ell} \geq 0 \quad \forall i_{dq} \in \mathbb{R}^2.$$

Another relevant aspect is the effect of $\omega_{el}(t)$ in the controller (12) and in the error dynamics (13). For $\omega_{el}(t) = 0$, the error of the dynamic compensator $e_2(t)$ is constant and does not converge to zero. Nonetheless, its convergence is not needed since in this scenario, the cross-coupling term does not affect the dynamics of the regulation error $e_1(t)$. Therefore, the important case is when $\omega_{el}(t)$ does not stay in zero. From a formal perspective, due to the employed method of proof, we need to exclude the cases where $\omega_{el}(t)$ crosses zero or where it converges asymptotically to this value. This restriction is formulated in Assumption 4. We remark that from a practical perspective this assumption is very reasonable, since a zero crossing represents a change in the direction of rotation.

Assumption 4. There exist positive constants $\omega_{\max} \geq \omega_{\min} > 0$ such that $\omega_{\max} \geq |\omega_{el}(t)| \geq \omega_{\min}$ for all $t \geq 0$.

To establish our main stability result, we introduce the Lyapunov function candidate
$$V(e,t) = e^\top P(t)e, \qquad (14)$$
with
$$P(t) = \begin{bmatrix} p_1 L_{dq}(t) & -\frac{1}{(r_s + k_1)k_2}L_{dq}(t)\mathbf{J} \\ -\frac{1}{(r_s + k_1)k_2}\mathbf{J}^\top L_{dq}(t) & \frac{p_1}{k_2}\mathbf{I}_2 \end{bmatrix}, \qquad (15)$$
where $p_1 > 0$ is a design parameter and $k_1 > 0$ as well as $k_2 > 0$ are the gains of the control law in (12). Some important properties of V are given in the next lemma, whose proof is given in in Appendix A.

Lemma 5. For every positive k_1 and k_2 and $L_{dq}(i_{dq})$ satisfying Assumption 1, there exist a large enough $p_1 > 0$, such that the function V defined in (14) satisfies the bounds $\rho_2\|e\|^2 \geq V(e,t) \geq \rho_1\|e\|^2$ for all $e \in \mathbb{R}^4$ and $t \geq 0$ for some constants $\rho_2 \geq \rho_1 > 0$.

We are now in the position to show that the control law in (12) provides a solution to Problem 2 for any positive controller gains k_1 and k_2.

Theorem 6. Consider Problem 2, the proposed controller in (12) and the error dynamics (13). Under Assumptions 3 and 4 and for any positive controller gains k_1 and k_2, the origin of the system (13) is locally uniformly exponentially stable. Furthermore, consider the ball defined by
$$\mathcal{B}_r(0) = \left\{ e \in \mathbb{R}^4, \|e\| \leq r = \frac{\rho_1}{\bar{\ell}\rho_2}c(k_1, k_2) \right\}, \qquad (16)$$
where the constants ρ_1 as well as ρ_2 are given in Lemma 5 and c is a positive constant that depends on the controller gains. Then, any error trajectory starting in $\mathcal{B}_r(0)$ converges to zero exponentially fast.

Theorem 6 shows that despite the variations in the inductances and that the controller (12) does not possess information about them, exponential tracking of the reference can be achieved. This is true even for non-constant $\omega_{el}(t)$. Another important point is that the radius r of the ball $\mathcal{B}_r(0)$ is inversely proportional to the upper bound $\bar{\ell}$ on the size of the gradients of the inductances with respect to the current. For example, if the machine is operated close to the saturation region of the machine iron, a small parameter $\bar{\ell}$ and, hence, a large radius r of the ball $\mathcal{B}_r(0)$ can be expected.

Furthermore, for constant inductances the region of attraction becomes the full error space, as is shown in Corollary 7 below. This represents a significant advantage even in the nominal case, since for implementing the controller in (12), the values of the inductances are not needed.

Corollary 7. Consider Problem 2 with the controller proposed in (12) and the error dynamics (13). Under Assumption 4 and Assumption 3 with $\bar{\ell} = 0$ for all $i_{dq} \in \mathbb{R}^2$, i.e. assuming a constant inductance matrix L_{dq}, $e(t) = 0$ is globally uniformly exponentially stable for any $k_1 > 0$ and $k_2 > 0$.

The proofs of Lemma 5, Theorem 6 and Corollary 7 are given in Appendix A.

4. SIMULATION EXAMPLE

In order to illustrate the advantages of the proposed control, we compare it with the standard PI-control, see (Du and Yu, 2007; Liu et al., 2018), in simulation. To provide a realistic scenario, the values given for the flux linkages and the inductances in (Stumberger et al., 2003) (Figures 9, 14, 18, 21, 24, 27) are used and evaluated in LUTs in the software `Matlab/Simulink`. Further model parameters were chosen in order to represent realistic values based on (Stumberger et al., 2003; Zaky, 2011; Tarczewski et al., 2018; Carpiuc et al., 2011) and are given in Table 1. To generate $\omega_{el}(t)$, the dynamical model (2) is used with $\omega_{el}(0) = 200$ [rad/s] and $T_L = 0.3$ [Nm]. With respect to the controllers, the gains of the proposed one

Table 1. Parameters of the IPMSM

Parameter	Value
Rated power (P_n)	0.676 kW
Rated phase current (I_s)	1.49 A
Number of poles ($2p$)	4
Rated speed (n_r)	2000 rev/min
Moment of inertia (J)	0.01 kg·m^2
Viscous friction coefficient (β)	0.007 kg·m^2/s
Nominal stator resistance (r_s)	1 Ω
Nominal flux linkage established by PM ($\lambda^\top$)	[0.15, 0] Vs

Fig. 1. Tracking of the d component of the current in per unit by the proposed algorithm (12) and the PI-control.

Fig. 2. Tracking of the q component of the current in per unit by the proposed algorithm (12) and the PI-control.

Fig. 3. Tracking error of the d component of the current in per unit by the proposed algorithm (12) and the PI-control.

(12) were selected as $k_1 = 300$ and $k_2 = 5$. In the case of the PI-control, the gains were selected as $k_p = 280$ and $k_i = 20$. The parameters of the controllers were chosen with keeping a realistic physical high voltage limit (ISO 6469-3) of the power supply in mind. Given that the PI-control requires the nominal values of the inductances, their values at zero current were used. This corresponds to

$$L_{dq} = \begin{bmatrix} 0.174 & 0.002 \\ 0.008 & 0.31 \end{bmatrix} \text{[H]}.$$

Finally, as a reference for the currents, the following piecewise constant function is selected:

$$\left(i_{dq}^{\text{ref}}\right)^\top \text{[A]} = \begin{cases} [-1.5, 1.5] & t \in [0, 0.04) \text{ [s]} \\ [-0.5, 0.5] & t \in [0.04, 0.08) \text{ [s]} \\ [-2, 2] & t \in [0.08, 0.12) \text{ [s]} \\ [-0.5, 0.5] & t \in [0.12, 0.16) \text{ [s]} \\ [-1, 1] & t \in [0.16, \infty) \text{ [s]} \end{cases}.$$

The results of the simulation are shown in Figures 1 - 6 and the corresponding variation of the inductances during the tracking process of the currents with the proposed algorithm (12) are given in Figures 7 - 8. In the simulation also the case of a short overload operation is included, which means that $i_q/I_s > 1$ and $-i_d/I_s > 1$. As can be seen from Figures 1 - 4, the proposed controller (12) achieves the correct tracking of the constant references, while the PI-control exhibits a steady-state error. In Figures 5 - 6 it can be seen that, compared to the PI-control, the proposed controller is also able to completely compensate the negative influence of the flux-linkage dependant cross-coupling term. In this context it is important to remark that for implementing the proposed controller, there is no need to have any information about the values of the inductances. In the case of the PI-control, the steady-state error goes up to 6% of the commanded current reference in the d-axis and up to 17% for the q-axis. This was expected since the feed-forward term is incorrect as soon as the inductances do not correspond to their nominal values. This mismatch is further amplified by $\omega_{\text{el}}(t)$. Thus, the performance of the PI-control deteriorates when the machine is operated at higher speeds. All these drawbacks are avoided with the proposed controller, demonstrating its superior properties compared to the usual PI-control scheme.

5. CONCLUSIONS

In this paper the problem of current control of IPMSMs is addressed. In those machines it is highly necessary to explicitly consider the variations of the machine inductances across the whole operation range in order to ensure a well-performing control. Motivated by this, a new current control on the basis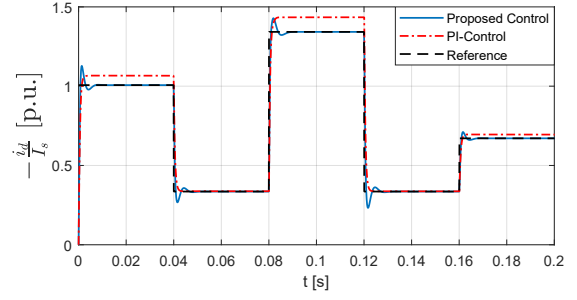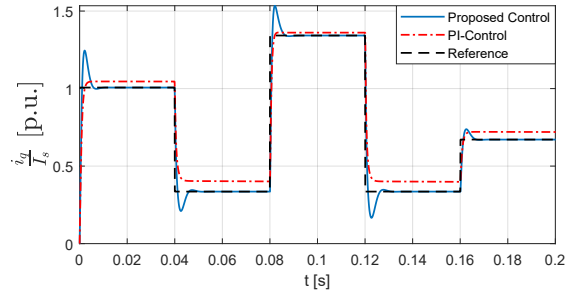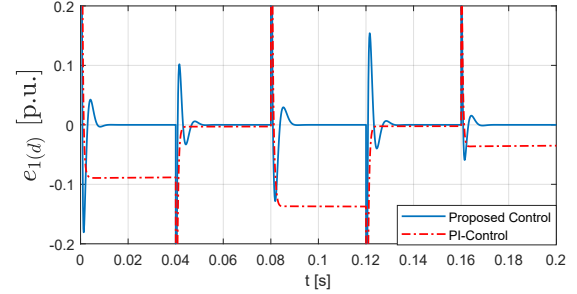 of the internal model principle is presented, which guarantees exponential tracking of the current references without requiring precise knowledge of the varying machine inductances. This is possible, because it is recognized that the main disturbance to the system follows a dynamical model, which is then used to design a dynamic compensator. The stability analysis of the resulting closed-loop system is carried out using standard Lyapunov stability theory. In addition, it is shown that the region for which the convergence of the regulation error is ensured, can be estimated by a ball, whose radius increases inversely proportional to the rate of change of the machine inductances under some reasonable assumptions. In contrast, it is shown in simulation that the inductance variations have a significant impact on the performance of the usual PI-based current control, which uses an inductance-dependant feed-forward term to eliminate the
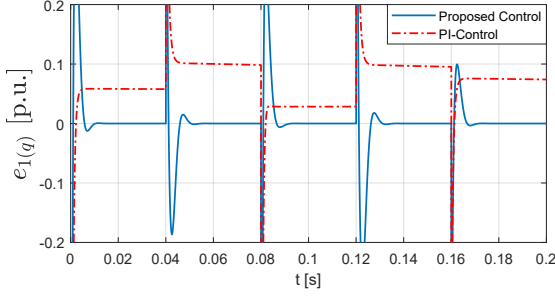
Fig. 4. Tracking error of the q component of the current in per unit by the proposed algorithm (12) and the PI-control.
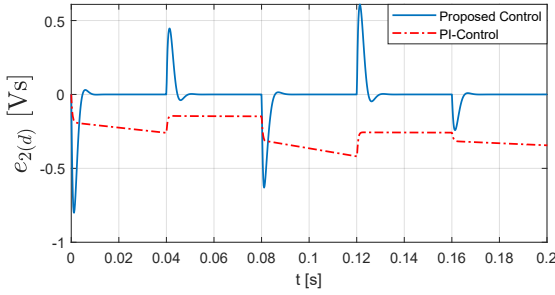

Fig. 5. Dynamical compensation error of the d component of the flux-linkage by the proposed algorithm (12) and the PI-control.
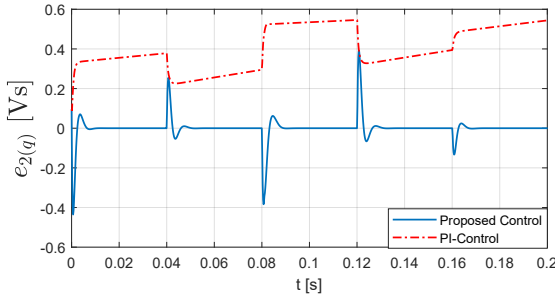

Fig. 6. Dynamical compensation error of the q component of the flux-linkage by the proposed algorithm (12) and the PI-control.

cross-couplings between the machine axes. Hence, slight deviations from the nominal inductance values result in a steady-state error in the tracking of the current references. On the contrary, when using the proposed control algorithm, the closed-loop system is rendered insensitive against variations in the machine inductances, which is a major advantage compared to the PI-based current control. This property makes costly practices to determine the inductance variations unnecessary.

In future work, the effect of zero crossings of $\omega_{\text{el}}(t)$ on the closed-loop stability will be analyzed. Another interesting direction of research is to investigate the behavior of the proposed control, when it is connected to the outer speed control loop, since the current references are usually coming from an optimization task done in the superordinate loop.
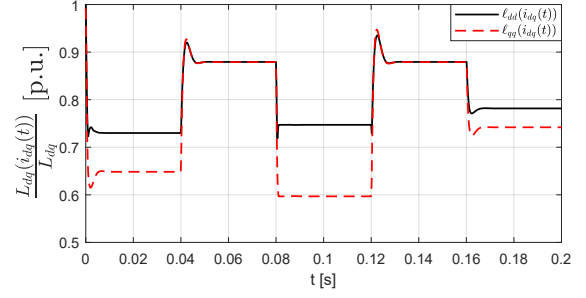

Fig. 7. Variation of the self inductances in per unit during the tracking process of the currents with the proposed algorithm (12).
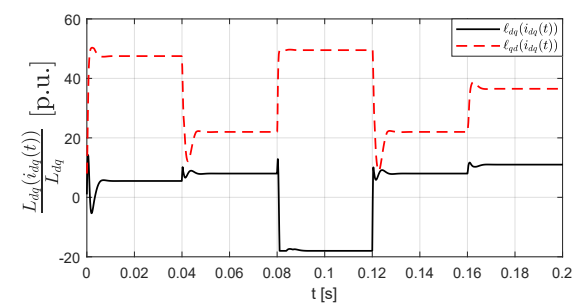

Fig. 8. Variation of the cross-coupling inductances in per unit during the tracking process of the currents with the proposed algorithm (12).

Appendix A. PROOF OF THE CLAIMS

A.1 Proof of Lemma 5

In order to show that the bounds over V hold, it will be shown that the matrix $P(t)$ satisfies $\rho_2 \mathbf{I}_4 \geq P(t) \geq \rho_1 \mathbf{I}_4 > 0$ for all $t \geq 0$. First, using the Schur complement of $P(t)$, it can be shown that for any $p_1 > \eta_1$, $P(t) > 0$ with

$$\eta_1 = \frac{\alpha_1}{(k_1 + r_s)\sqrt{\alpha_2 k_2}},$$

and α_1 and α_2 given in Assumption 1. Now, for any fixed p_1 satisfying the previous condition, a lower bound of the form $P(t) - \rho_1 \mathbf{I}_4 \geq 0$ can be determined with the help of the Schur complement

$$\chi_{\rho_1} = p_1 L_{dq}(t) - \rho_1 \mathbf{I}_2 - \frac{1}{k_2(p_1 - k_2\rho_1)(k_1 + r_s)^2} L_{dq}^2(t)$$

$$\geq \left(p_1 \alpha_2 - \rho_1 - \frac{\alpha_1^2}{k_2(p_1 - k_2\rho_1)(k_1 + r_s)^2} \right) \mathbf{I}_2.$$

Then, χ_{ρ_1} is positive for any

$$0 < \rho_1 \leq \frac{p_1(1 + \alpha_2 k_2)}{2k_2} - \sqrt{\frac{(p_1(1 + \alpha_2 k_2))^2}{4k_2^2} + \frac{\alpha_1^2}{k_2^2(k_1 + r_2)^2} - \frac{\alpha_2 p_1^2}{k_2}},$$

showing the existence of the lower bound $P(t) \geq \rho_1 \mathbf{I}_4$. In the case of the upper bound, it is easy to see that for every fixed p_1, an appropriate ρ_2 exists, since $L_{dq}(t)$ is bounded by Assumption 1. This upper bound can be determined with the Schur complement of the difference $\rho_2 \mathbf{I}_4 - P(t) \geq 0$

$$\chi_{\rho_2} = \rho_2 \mathbf{I}_2 - p_1 L_{dq}(i_{dq}(t)) - \frac{L_{dq}^2(i_{dq}(t))}{(\rho_2 k_2 - p_1)(r_s + k_1)^2 k_2},$$
$$\geq \left(\rho_2 - p_1 \alpha_1 - \frac{\alpha_1^2}{(\rho_2 k_2 - p_1)(r_s + k_1)^2 k_2} \right) \mathbf{I}_2.$$

In this case, χ_{ρ_2} is positive for

$$\rho_2 \geq \frac{p_1(1 + \alpha_1 k_2)}{2k_2} + \sqrt{\frac{(p_1(1 + \alpha_1 k_2))^2}{4k_2^2} + \frac{\alpha_1^2}{k_2^2(k_1 + r_s)^2} - \frac{\alpha_1 p_1^2}{k_2}} > 0.$$

Therefore, positive constants ρ_1 and ρ_2 that bound $V(e, t)$ exist.

A.2 Proof of Theorem 6

With the result from Lemma 5, it is clear that $V(t, e)$ in (14) can be taken as a Lyapunov function candidate. Its derivative along the trajectories of (13) results in

$$\dot{V}(t) \leq -e^\top(t)\Big(Q(t) - \dot{P}(t)\Big)e(t), \qquad \text{(A.1)}$$

with $-Q(t) = P(t)A(t) + A^\top(t)P(t)$, $A(t)$ as in (13) and $Q(t)$ given by

$$Q(t) = \begin{bmatrix} Q_{11}(t) & Q_{12}(t) \\ Q_{12}^\top(t) & Q_{22}(t) \end{bmatrix},$$

$$Q_{11}(t) = 2p_1(r_s + k_1)\mathbf{I}_2 - 2\frac{|\omega_{\text{el}}(t)|}{(r_s + k_1)}L_{dq}(t),$$

$$Q_{12}(t) = -\frac{|\omega_{\text{el}}(t)|}{(r_s + k_1)k_2}L_{dq}(t) - \frac{1}{k_2}\mathbf{J}, \qquad \text{(A.2)}$$

$$Q_{22}(t) = 2\frac{|\omega_{\text{el}}(t)|}{(r_s + k_1)k_2}\mathbf{I}_2.$$

The time derivative of $P(t)$ can be computed as

$$\dot{P}(t) = \begin{bmatrix} p_1 \dot{L}_{dq}(t) & -\dfrac{\text{sign}(\omega_{\text{el}}(t))}{(r_s + k_1)k_2}\dot{L}_{dq}(t)\mathbf{J} \\ -\dfrac{\text{sign}(\omega_{\text{el}}(t))}{(r_s + k_1)k_2}\mathbf{J}^\top \dot{L}_{dq}(t) & 0 \end{bmatrix}.$$

To show the negative definiteness of $\dot{V}(t)$, it can be seen from (A.1) that bounds over $Q(t)$ and $\dot{P}(t)$ are needed. These are derived next.

Let $q \in (0, 2\omega_{\min}/(k_2(r_s + k_1)))$, then $Q(t) - q\mathbf{I}_4 \geq 0$ can be ensured if the Schur complement

$$\chi_Q = 2p_1(r_s + k_1 - q)\mathbf{I}_2 - \frac{2|\omega_{\text{el}}(t)|}{(r_s + k_1)}L_{dq}(t)$$
$$- \frac{k_2(r_s + k_1)}{2|\omega_{\text{el}}(t)| - qk_2(r_s + k1)}Q_{12}(t)Q_{12}^\top(t)$$
$$\geq \left(2p_1(r_s + k_1 - q) - \frac{2\omega_{\max}\alpha_1}{(r_s + k_1)} \right.$$
$$\left. - \frac{2k_2(r_s + k_1)}{2\omega_{\min} - qk_2(r_s + k_1)}\left(\frac{\omega_{\max}^2 \alpha_1^2}{k_2^2(r_s + k_1)^2} + \frac{1}{k_2^2} \right) \right)\mathbf{I}_2$$

is positive. This happens for $p_1 \geq \eta_2$ with

$$\eta_2 = \frac{2\alpha_1 \omega_{\max} + q(k_1 + r_s)}{2(k_1 + r_s)^2} + \frac{\alpha_1^2 \omega_{\max}^2 + (k_1 + r_s)^2}{k_2(k_1 + r_s)^2(2\omega_{\min} - qk_2(k_1 + r_s))}.$$

To bound $\dot{P}(t)$, we need to bound $\dot{L}_{dq}(t)$ first. This can be done by analysing the time derivative of each of its components, i.e.,

$$\|\dot{\ell}_{ij}(t)\| \leq \bar{\ell}\|\dot{e}_1(t)\| \leq \bar{\ell}\frac{\max\{k_1, \omega_{\max}\}}{\alpha_2}\|e(t)\|.$$

Define $\kappa = \max\{k_1, \omega_{\max}\}/\alpha_2$. Then, it follows that $\|\dot{L}_{dq}(t)\| \leq 2\bar{\ell}\kappa\|e(t)\|$. To continue, the bound for $\dot{P}(t)$ can be developed by finding a scalar function $r(e)$, such that $r(e)\mathbf{I}_4 - \dot{P}(t) \geq 0$. This is done with the help of the Schur complement of the difference

$$\chi_{\dot{P}} = r(e)\mathbf{I}_2 - p_1 \dot{L}_{dq}(t) - \frac{1}{r(e)(r_s + k_1)^2 k_2^2}\dot{L}_{dq}^2(t),$$
$$\geq \left(r(e) - 2\bar{\ell}\kappa p_1\|e(t)\| - \frac{4\bar{\ell}^2 \kappa^2\|e(t)\|^2}{r(e)(r_s + k_1)^2 k_2^2} \right)\mathbf{I}_2.$$

From here, it follows that $\chi_{\dot{P}} \geq 0$ if

$$r(e) \geq \left(p_1 + \sqrt{p_1^2 + \frac{4}{(r_s + k_1)^2 k_2^2}} \right)2\bar{\ell}\kappa\|e(t)\|. \qquad \text{(A.3)}$$

With the bounds for $Q(t)$ and $\dot{P}(t)$ in mind, the time derivative of V can be bounded as

$$\dot{V}(t) \leq -q\|e(t)\|^2 + r(e)\|e(t)\|^2.$$

Select $r(e)$ as

$$r(e) = 2\bar{\ell}\kappa \left(p_1 + \frac{1}{k_2(k_1 + r_s)} \right)\|e(t)\|,$$

which satisfies (A.3). Then $\dot{V}(t) < 0$ for

$$\|e(t)\| \leq \frac{c(k_1, k_2)}{\bar{\ell}} = \frac{qk_2(k_1 + r_s)}{2\bar{\ell}\kappa(1 + p_1 k_2(k_1 + r_2))}$$
$$= \frac{q\alpha_2 k_2(k_1 + r_s)}{2\bar{\ell}\max\{k_1, \omega_{\max}\}(1 + p_1 k_2(k_1 + r_2))}, \qquad \text{(A.4)}$$

proving that $e(t) = 0$ is a locally uniformly exponentially stable equilibrium point (Khalil, 2002)[Theo. 4.10]. Furthermore, in light of (Khalil, 2002)[Theo. 4.9] and the bounds over V in Lemma 5, any error trajectory starting in the ball $\mathcal{B}_r(0)$ given in (16) will converge to zero.

A.3 Proof of Corollary 7

Under the assumptions in the corollary, L_{dq} is a constant, positive definite matrix. Thus, $\dot{P}(t) = 0$ in (A.1). A lower and constant bound for the resulting matrix $Q(t)$ can be found in a similar manner as done in Appendix A.2. Then $Q(t) \geq q\mathbf{I}_4$, and

$$\dot{V}(t) \leq -q\|e(t)\|^2 < 0,$$

showing that $e(t) = 0$ is globally uniformly exponentially stable (Khalil, 2002)[Theo. 4.10].

REFERENCES

Blaschke, F. (1972). The principle of field orientation applied to the new transvector closed-loop control system for rotating field machines. *Siemens-Rev.*, 39, 217–220.

Carpiuc, S., Patrascu, D., and Lazar, C. (2011). Optimal torque control of the interior permanent magnet synchronous machine. In *2011 XXIII International Symposium on Information, Communication and Automation Technologies*, 1–8.

Chan, C.C. and Chau, K.T. (2001). *Modern Electric Vehicle Technology*. Oxford University Press.

Choi, J., Nam, K., Bobtsov, A.A., and Ortega, R. (2019). Sensorless control of ipmsm based on regression model. *IEEE Trans. Power Electron.*, 34(9), 9191–9201.

Du, C. and Yu, G. (2007). Optimal pi control of a permanent magnet synchronous motor using particle swarm optimization. In *Second International Conference on Innovative Computing, Informatio and Control (ICICIC 2007)*, 255–255.

Francis, B. and Wonham, W. (1976). The internal model principle of control theory. *Automatica*, 12(5), 457 – 465.

Gai, Y., Kimiabeigi, M., Chong, Y.C., Widmer, J., Deng, X., Popescu, M., Goss, J., Staton, D., and Steven, A. (2018). Cooling of automotive traction motors: Schemes, examples and computation methods- a review. *IEEE Trans. Ind. Electron.*, PP, 1–1.

Gyu-Hong Kang, Jung-Pyo Hong, Gyu-Tak Kim, and Jung-Woo Park (2000). Improved parameter modeling of interior permanent magnet synchronous motor based on finite element analysis. *IEEE Trans. Magn*, 36(4), 1867–1870.

Hosseini, S.H. and Tabatabaei, M. (2017). Ipmsm velocity and current control using mtpa based adaptive fractional order sliding mode controller. *Engineering Science and Technology, an International Journal*, 20(3), 896 – 908.

Jie Huang and Ching-Fang Lin (1993). Internal model principle and robust control of nonlinear systems. In *Proceedings of 32nd IEEE Conference on Decision and Control*, 1501–1506 vol.2.

Khalil, H. (2002). *Nonlinear Systems*. Prentice–Hall, New Jersey, third edition.

Kim, H., Lee, Y., Sul, S., Yu, J., and Oh, J. (2018). Online MTPA Control of IPMSM for Automotive Applications Based on Robust Numerical Optimization Technique. In *2018 IEEE Transportation Electrification Conference and Expo (ITEC)*, 442–447.

Lee, K., Ha, J., and Simili, D.V. (2019). Analysis and suppression of slotting and cross-coupling effects on current control in pm synchronous motor drives. *IEEE Trans. Power Electron.*, 34(10), 9942–9956.

Lemmens, J., Vanassche, P., and Driesen, J. (2015). Pmsm drive current and voltage limiting as a constraint optimal control problem. *IEEE Trans. Emerg. Sel. Topics Power Electron.*, 3(2), 326–338.

Li, S., Han, D., and Sarlioglu, B. (2017). Modeling of interior permanent magnet machine considering saturation, cross coupling, spatial harmonics, and temperature effects. *IEEE Trans. Transport. Electrific.*, 3(3), 682–693.

Liang, P., Pei, Y., Chai, F., and Zhao, K. (2016). Analytical calculation of d- and q-axis inductance for interior permanent magnet motors based on winding function theory. *Energies*, 9, 580.

Liu, B., Zhao, Y., and Hu, H.Z. (2018). Structure-variable sliding mode control of interior permanent magnet synchronous motor in electric vehicles with improved flux-weakening method. *Advances in Mechanical Engineering*, 10(1).

Liu, J., Gong, C., Han, Z., and Yu, H. (2018). Ipmsm model predictive control in flux-weakening operation using an improved algorithm. *IEEE Trans. Ind. Electron.*, 65(12), 9378–9387.

Meessen, K., Thelin, P., Soulard, J., and Lomonova, E. (2008). Inductance calculations of permanent-magnet synchronous machines including flux change and self- and cross-saturations. *IEEE Trans. Magn.*, 44, 2324 – 2331.

Momoh, O.D. and Omoigui, M.O. (2009). An overview of hybrid electric vehicle technology. In *2009 IEEE Vehicle Power and Propulsion Conference*, 1286–1292.

Mou, X., Zhang, Y., Jiang, J., and Sun, H. (2019). Achieving low carbon emission for dynamically charging electric vehicles through renewable energy integration. *IEEE Access*, 7, 118876–118888.

Ortega, R., Monshizadeh, N., Monshizadeh, P., Bazylev, D., and Pyrkin, A. (2018). Permanent magnet synchronous motors are globally asymptotically stabilizable with pi current control. *Automatica*, 98, 296 – 301.

Pillay, P. and Krishnan, R. (1988). Modeling of permanent magnet motor drives. *IEEE Trans. Ind. Electron.*, 35(4), 537–541.

Schröder, D. (2015). *Elektrische Antriebe - Regelung von Antriebssystemen*. Springer, Vieweg, Berlin, Heidelberg.

Stumberger, B., Stumberger, G., Dolinar, D., Hamler, A., and Trlep, M. (2003). Evaluation of saturation and cross-magnetization effects in interior permanent-magnet synchronous motor. *IEEE Trans. Ind Appl.*, 39(5), 1264–1271.

Sulaiman, E., Kosaka, T., and Matsui, N. (2011). A new structure of 12slot-10pole field-excitation flux switching synchronous machine for hybrid electric vehicles. In *Proceedings of the 2011 14th European Conference on Power Electronics and Applications*, 1–10.

Sun, J., Luo, X., and Ma, X. (2018). Realization of maximum torque per ampere control for ipmsm based on inductance segmentation. *IEEE Access*, 6, 66088–66094.

Tarczewski, T., Skiwski, M., Niewiara, L., and Grzesiak, L. (2018). High-performance pmsm servo-drive with constrained state feedback position controller. *Bulletin of the Polish Academy of Sciences, Technical Sciences*, 66. doi:10.24425/119058.

Wallscheid, O., Peters, W., and Böcker, J. (2012). A precise open-loop torque control for an interior permanent magnet synchronous motor (ipmsm) considering iron losses. *IECON Proceedings*.

Yu, L., Zhang, Y., and Huang, W. (2017). Accurate and efficient torque control of an interior permanent magnet synchronous motor in electric vehicles based on hall-effect sensors. *Energies*, 10, 410.

Zaky, M. (2011). Adaptive and robust speed control of interior permanent magnet synchronous motor drives. *Electrical Engineering - ELECTR ENG*, 94.

Zhu, Z.Q. and Howe, D. (2007). Electrical machines and drives for electric, hybrid, and fuel cell vehicles. *Proceedings of the IEEE*, 95(4), 746–765.